

"This is the peer reviewed version of the following article: **Supramolecular Water Oxidation with Ru-bda Based Catalysts**, which has been published in final form at <http://onlinelibrary.wiley.com/doi/10.1002/chem.201405144/abstract> This article may be used for non-commercial purposes in accordance with [Wiley Terms and Conditions for Self-Archiving](#)."

## Supramolecular Water Oxidation with Ru-bda Based Catalysts

Craig J. Richmond,<sup>[a]</sup> Roc Matheu,<sup>[a]</sup> Albert Poater,<sup>[b]</sup> Laura Falivene,<sup>[c]</sup> Jordi Benet-Buchholz,<sup>[a]</sup> Xavier Sala,<sup>\*,[d]</sup> Luigi Cavallo,<sup>\*,[c]</sup> and Antoni Llobet,<sup>\*,[a],[d]</sup>

**Abstract:** Extremely slow and extremely fast new water oxidation catalysts based on the Ru-bda systems are reported with turnover frequencies in the range of 1 and 900 cycles/s respectively. Detailed analyses of the main factors involved in the water oxidation reaction have been carried out and are based on a combination of reactivity tests, electrochemical experiments and DFT calculations. These analyses, give a convergent interpretation that generates a solid understanding of the main factors involved in the water oxidation reaction, which in turn allows the design of catalysts with very low energy barriers in all the steps involved in the water oxidation catalytic cycle. We show that for this type of system  $\pi$ -stacking interactions are the key factors that influence reactivity and by adequately controlling them we can generate exceptionally fast water oxidation catalysts.

Today a transition from fossil to solar fuels is needed in order to provide us with a clean and sustainable energy model. A viable option to achieve this challenge is to split water with sun light, however,

before this can be realized, one of the key issues that needs to be understood and mastered is water oxidation catalysis. In this respect significant progress has been accomplished over the last five years, mainly based on molecular transition metal complexes.<sup>[1]</sup> Among the best water oxidation catalysts (WOCs) reported today are dinuclear Ru complexes that make O-O bonds via a water nucleophilic attack mechanism (WNA)<sup>[2]</sup> and a family of mononuclear Ru complexes based on the tetradentate ligand [2,2'-bipyridine]-6,6'-dicarboxylic acid (H<sub>2</sub>bda; see Scheme 1 for the ligand structures described in this paper) that make O-O bonds via a bimolecular Ru-oxo coupling mechanism (I2M).<sup>[3]</sup> Spectacular performances both in terms of maximum turnover frequencies ( $TOF_{max}$ ) and turnover numbers (TONs) have been reported, with [Ru(bda)(isoq)<sub>2</sub>], **1**, (isoq = isoquinoline), which has a  $TOF_{max} \approx 300 \text{ s}^{-1}$ , comparable to that of the oxygen evolving systems of photosystem II (OEC-PSII). Complex **1** has been modified by introducing additional functionalities at the axial monodentate pyridyl ligands, allowing it to be anchored on carbon nano-tubes or oxide surfaces, both of which have proved to be useful methods to create efficient photoanodes for electrochemical cells.<sup>[4]</sup> For the success of the latter it is crucial that the water oxidation catalysis is sufficiently fast so that it can compete favorably with the potential non-productive and deactivating reactions. Thus a detailed mechanistic analysis at a molecular level is essential in order to gain knowledge about the origin of the activation barriers that are responsible for the rate determining step (rds). For the particular case of [Ru(bda)(Isoq)<sub>2</sub>], **1**, it was found that the rds, under catalytic conditions at pH = 1.0, involves the dimerization of the complex at the formal oxidation

[a] Craig J. Richmond, Roc Matheu, Dr. Jordi Benet-Buchholz, Prof. Antoni Llobet  
Institute of Chemical Research of Catalonia (ICIQ)  
Av. Països Catalans 16 – 43007, Tarragona, Spain  
E-mail: allobet@iciq.es

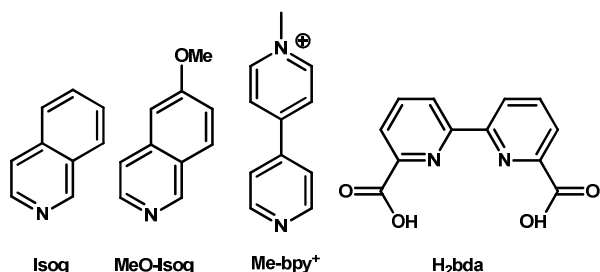
[b] Dr. Albert Poater  
Institut de Química Computacional i Catàlisi and Departament de Química, Universitat de Girona, Campus de Motilivi, E-17071 Girona, Spain

[c] Dr. Laura Falivene, Prof. Luigi Cavallo  
KAUST Catalysis Center, Chemical and Life Sciences and Engineering, King Abdullah University of Science and Technology, Thuwal 23955-6900, Saudi Arabia.

[d] Dr. Xavier Sala, Prof. Antoni Llobet  
Departament de Química, Universitat Autònoma de Barcelona, Cerdanyola del Vallès, 08193 Barcelona, Spain.

Supporting information for this article is given via a link at the end of the document and it contains additional experimental, spectroscopic, electrochemical, crystallographic (cif files; CCDC 1014178) and DFT data.

state V generating a peroxy dinuclear complex, thus following a mechanism that involves the interaction of two M-O units (12M). Further one electron oxidation of the peroxide generates the species responsible for the dioxygen release.<sup>[3b]</sup>



**Scheme 1.** Ligand structures and abbreviations.

Attempts to improve the performance of Ru-bda complexes include the exertion of electronic perturbations at the metal site via sigma and  $\pi$ -interactions through substituents at the 4-position of the axial groups.<sup>[3]</sup> For example, the complex containing ethyl isonicotinate, [Ru(bda)(4-COOEt-py)<sub>2</sub>], **2**, is significantly faster than the 4-methyl pyridine complex [Ru(bda)(4-Me-py)<sub>2</sub>], **3**, with an impressive  $TOF_{max}$  of 119 s<sup>-1</sup>. Another important factor that improves reaction rates is the  $\pi$ -stacking interaction of the axial ligands, as can be deduced by comparing the  $TOF_{max}$  of **1** (c.a. 300 s<sup>-1</sup>) with that of **3** (c.a. 32 s<sup>-1</sup>), which under similar conditions is about one order of magnitude slower.

In this work two new Ru-bda complexes; [Ru(bda)(L)<sub>2</sub>]<sup>n+</sup>, (L = MeO-isoq, n = 0, **4**; L = Me-bpy<sup>+</sup>, n = 2, **5**(PF<sub>6</sub>)<sub>2</sub>) are reported in order to further explore the benefit of the  $\pi$ -stacking interaction for this type of catalyst. Whilst the complex containing the MeO-isoq was expected to lead to favorable  $\pi$ -stacking effects in water, the opposite was expected for that containing the Me-bpy<sup>+</sup> ligand due to its cationic nature and the non-parallel orientation of the pyridyl rings.

Ru(bda) WOCs **4** and **5** were synthesized following the previously reported one-pot method,<sup>[3a,4b]</sup> mixing [RuCl<sub>2</sub>(DMSO)<sub>4</sub>] with the aryl axial ligands and bda<sup>2-</sup> in

MeOH and heating to reflux. The as prepared compounds were characterized by standard electrochemical and spectroscopic techniques (for full experimental details and spectra see ESI). An X-ray structure of **4** is presented in Figure 1, the bonding parameters are typical for a Ru(II) d<sup>6</sup> low spin complex,<sup>[5]</sup> however, the most interesting feature of the X-ray analysis is its 3D packing, where strong  $\pi$ -stacking interactions can be clearly observed between the isoquinoline ligands (See Figure 1). Spiraling columns of three separate molecules form, with distances between  $\pi$ -systems in the range of 3.4-3.7 Å, thus providing precedence for the stacking interactions also proposed to be present during the catalytic cycle.

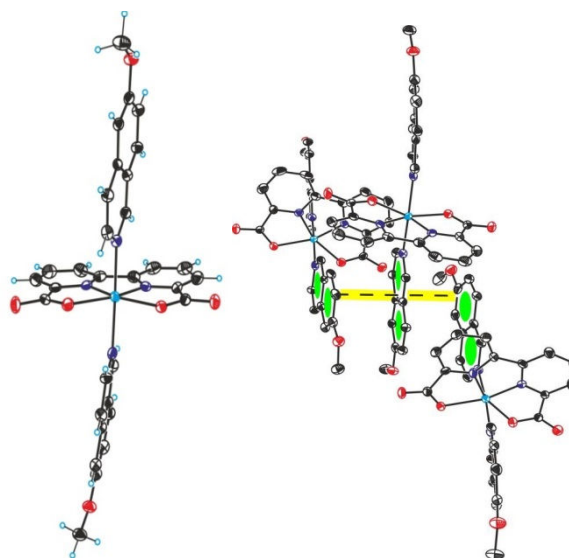


**Figure 1.** Left, Ortep view for the molecular X-ray structure of **4**. Ellipsoids are plotted at 50 % probability. Color codes: Ru, cyan; N, blue; O, red; C, black; H, light blue. Right, representation of the  $\pi$ -stacking observed in groups of three molecules. The distance between the aromatic rings is in the range 3.4-3.5 Å.

The electrochemical properties of **1**, **4** and **5** were investigated by means of cyclic voltammetry (CV) and differential pulse voltammetry (DPV) using the Hg/Hg<sub>2</sub>SO<sub>4</sub> as a reference electrode with the results shown in Figure 2 and Table 1 and the supporting

information. From these experiments it is found that the III/II redox potential is the one that suffers the strongest shift due to the electronic effects exerted by the axial ligands. On the other hand the IV/III and V/IV redox potentials are slightly modified. Ironically the most affected redox potential is irrelevant for the catalysis kinetics since the oxidation state II is not involved in the catalytic cycle, it acts only as a catalyst precursor to the oxidation state III that is the lowest oxidation state involved in the catalytic cycle.<sup>[3a]</sup> For complex **4**, the V/IV wave is associated with a large electrocatalytic current, as can be observed in the CV of Figure 2, whereas for complex **5** the current is practically identical to the blank, indicating that for the latter the catalysis, if it exists, is very slow. Since the potentials for the redox couples correlated to the catalytic cycles of both **4** and **5** are very similar to each other, it seems probable that the large difference in their reactivity is relevant to the intermolecular stacking associations.

The assessment of the complexes' activity towards water oxidation was further investigated chemically using Ce(IV) as a sacrificial oxidant at pH = 1.0, the results are reported in Figure 3 and Table 1. Manometric gas measurements were used to assess the activity for both the individual catalysts (**1**, **4** and **5**) and 1:1 mixtures of **4** and **5**. Online mass spectrometry and headspace analysis with a Clark electrode were used to confirm O<sub>2</sub> as the only component of the gas produced (see ESI Figures S27-28)

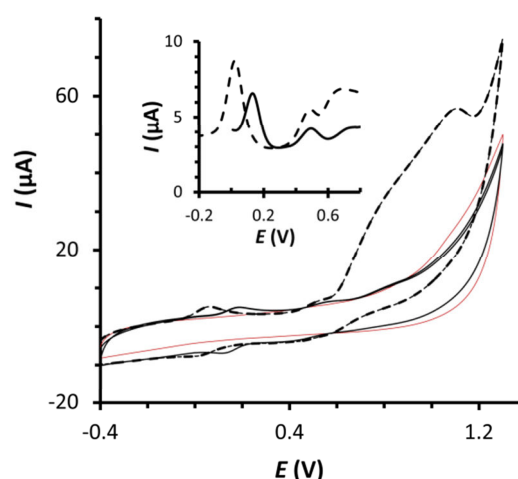


**Figure 2.** Cyclic voltammograms and DPV (inset) of **4** (dashed line, 0.32 mM), **5** (solid line, 0.32 mM) and bare glassy carbon electrode (red line) in a 0.1 M triflic acid solution containing 25% TFE. The scan rate was 100 mV/s and a glassy carbon electrode (0.07 cm<sup>2</sup>) was used as working, Pt mesh was used as counter and Hg/Hg<sub>2</sub>SO<sub>4</sub> (MSE) as reference electrodes.

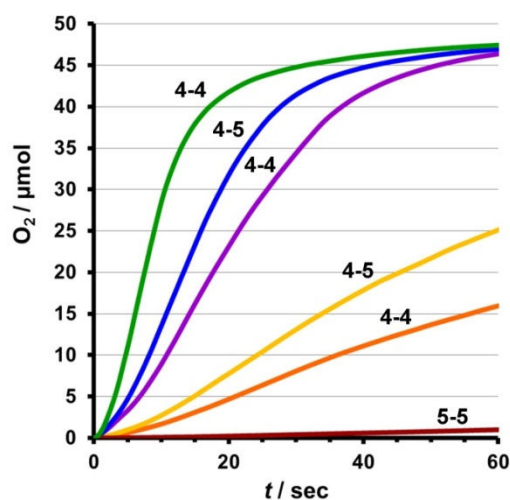


**Figure 3.** Oxygen evolution profile for Ru-bda catalysts **4** and **5** in varying catalyst ratios and concentrations, [CAN] = 0.1 M, in 2.0 mL 0.1 M triflic acid at 25 °C; [**4**] = 5.0 μM green, [**4**] = [**5**] = 2.5 μM blue, [**4**] = 2.5 μM purple, [**4**] = [**5**] = 1.25 μM yellow, [**4**] = 1.25 μM orange, [**5**] = 5.0 μM red.

Table 1 shows the impressive performance of the Ru-bda family of catalysts under different conditions at pH = 1.0. For instance in entry 3, complex **4** 5.0  $\mu\text{M}$ /Ce(IV) 100 mM (1/20000) generates oxygen at a maximum velocity ( $v_{\text{max}}$ ) of 3.81  $\mu\text{mol/s}$  ( $\text{TOF}_{\text{max}} = 381 \text{ s}^{-1}$ ) with basically 100% oxidative efficiency that illustrates the ruggedness of this family of catalysts.

**Table 1.** Reactivity and electrochemical parameters for Ru-bda catalysts.

Entry <sup>[a]</sup>	WOC	[WOC] / $\mu\text{M}$	[CeIV] / mM	$v_{\text{max}} / \mu\text{mol s}^{-1}$ <sup>[c]</sup>	$\text{TOF}_{\text{max}} / \text{s}^{-1}$ <sup>[c]</sup>	$E_{1/2}$ vs. NHE <sup>[d]</sup>	WOC	[WOC] / $\mu\text{M}$	[CeIV] / mM	$v_{\text{max}} / \mu\text{mol s}^{-1}$ <sup>[c]</sup>	$\text{TOF}_{\text{max}} / \text{s}^{-1}$ <sup>[c]</sup>	$E_{1/2}$ vs. NHE <sup>[d]</sup>			
9	1	2.5	100	0.637 $\pm 0.006$	127 $\pm 1$	0.70	1.17	1.38	10	1	5.0	100	2.56 $\pm 0.01$	256 $\pm 1$	
11	4+5	1.25+1.25	100	0.52 $\pm 0.07$	103 $\pm 3$				12	4+5	2.5+2.5	100	2.01 $\pm 0.07$	201 $\pm 7$	
1	4	1.25	100	0.320 $\pm 0.005$	130 $\pm 2$	0.67			13	4	50	350	23.07 $\pm 0.08$	923 $\pm 3$	
2	4	2.5	100	1.26 $\pm 0.01$	252 $\pm 2$	0.78			14	5	2.5	100	0.0055 $\pm 0.0002$	1.10 $\pm 0.02$	
3	4	5.0	100	3.81 $\pm 0.16$	381 $\pm 16$	0.78			15	5	5.0	100	0.0200 $\pm 0.0002$	2.00 $\pm 0.02$	
4 <sup>[b]</sup>	4	50	350	23.07 $\pm 0.08$	923 $\pm 3$	0.78			16	5	20	100	0.350 $\pm 0.008$	8.8 $\pm 0.2$	
5	5	2.5	100	0.0055 $\pm 0.0002$	1.10 $\pm 0.02$	0.78			17	1	1.25	100	0.104 $\pm 0.001$	41.8 $\pm 0.4$	
6	5	5.0	100	0.0200 $\pm 0.0002$	2.00 $\pm 0.02$	0.78			18	1	1.25	100	0.104 $\pm 0.001$	41.8 $\pm 0.4$	
7	5	20	100	0.350 $\pm 0.008$	8.8 $\pm 0.2$	0.78			19	1	1.25	100	0.104 $\pm 0.001$	41.8 $\pm 0.4$	
8	1	1.25	100	0.104 $\pm 0.001$	41.8 $\pm 0.4$	0.78			20	1	1.25	100	0.104 $\pm 0.001$	41.8 $\pm 0.4$	

[a] Headspace = 8.5 mL, Temperature = 25 °C, solvent = 3% TFE in 0.1 M triflic acid (2.0 mL), [CAN] = 0.1 M. [b] Headspace = 27.0 mL, Temperature = 25 °C, solvent = 3% TFE in 0.1 M triflic acid (0.5 mL), [CAN] = 0.35 M. [c] Calculations based on averaged data obtained from duplicate reactions. [d] III/II, IV/III and V/IV redox potentials respectively in V vs. NHE. Potentials converted from MSE. [e] data from reference 3b.

A kinetic analysis (see ESI Figure S24 and S25) of the reactivity of complexes **4** and **5** based on initial rates, maintaining the Ce(IV) concentration constant and varying the concentration of **4** and **5**, gives a second order behavior, which is again consistent with the fact that the stacking interactions are involved in the rate determining step.

It is also very interesting to point out that under identical conditions (entries 1-3 vs. 8-10), complex **4** containing the MeO substituted isoquinoline is about two to three times faster than the non-substituted isoquinoline complex, **1**. This can be attributed to a better stacking match in rds transition state (TS), due to the offset of the two Ru-bda moieties. In sharp contrast, under identical conditions, complex **5** containing the Me-bpy<sup>+</sup> ligand has maximum velocities that are 190 and 128 times slower than **4** and **1** respectively (see entries 3, 6 and 10). Clearly here the positive charge around the Me-bpy<sup>+</sup> ligand

outweighs the stacking effect and as a consequence lacks the low energy pathway for oxygen formation provided by the bimolecular mechanism is less favorable.

In order to extract further evidence regarding the nature of the  $\pi$ -stacking interaction 1:1 mixtures of complexes **4** and **5** were evaluated (see Figure 3. and Table 1 entries 11-12). Entry 11 shows that a 1.25  $\mu\text{M}$ :1.25  $\mu\text{M}$  combination of **4**:**5** and 100 mM Ce(IV) gives a maximum velocity of 0.52  $\mu\text{mol/s}$ . Combining this data with the rest of the table, the following considerations and conclusions can be extracted: i) Following a bimolecular pathway, three types of interactions can contribute to reach this rate; the **4**:**4**, the **4**:**5** or the **5**:**5**. The latter, as we have shown previously, is more than 2 orders of magnitude slower than the **4**:**4** and thus cannot significantly contribute to the final velocity observed; ii) If there was only the **4**:**4** type of interaction then the rate obtained should be 0.32  $\mu\text{mol s}^{-1}$ , similar to entry 1 of the Table. The fact that the rate observed is 0.52  $\mu\text{mol/s}$  clearly manifests the existence of a **4**:**5** interaction; iii) Assuming no contribution from the **4**:**4** interaction, then the maximum velocity for the **4**:**5** (1.25  $\mu\text{M}$ :1.25  $\mu\text{M}$ ) interaction would be 0.52  $\mu\text{mol/s}$ , and hence a  $TOF_{\text{max}}$  of 103  $\text{s}^{-1}$ ; iv) For the **4**:**4** (1.25  $\mu\text{M}$ :1.25  $\mu\text{M}$ ) interaction under these conditions (entry 2) a rate of 1.26  $\mu\text{mol s}^{-1}$  is observed, resulting in a  $TOF_{\text{max}}$  of 252  $\text{s}^{-1}$ .

If the activation energy in the rds is inversely proportional to the strength of the stacking interaction, then the rate of oxygen production should also follow this trend, which is what was observed for 1.25  $\mu\text{M}$ :1.25  $\mu\text{M}$  pairs of **4** and **5**, **4**:**4** > **4**:**5** >> **5**:**5** (1.26 > 0.52 >> --). A similar analysis with identical conclusions can be carried out by comparing the 2.5  $\mu\text{M}$  combination (entry 12, 3 and 6) giving the same trend, **4**:**4** > **4**:**5** >> **5**:**5** (3.81 > 2.01 >> 0.02).

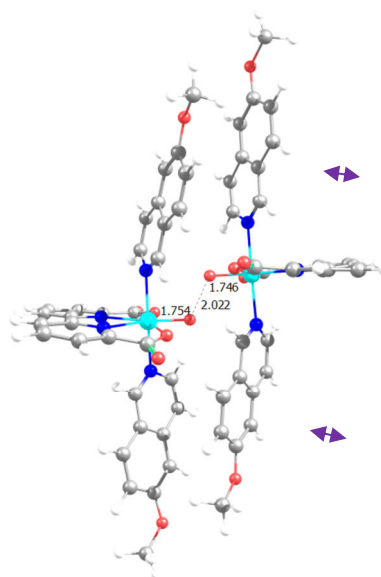


**Figure 4.** Calculated TS structure for the **4**:**4** dimer (distances in Å).

DFT calculations were performed to support the scenarios emerging from the experiments. Focusing on the O-O bond formation step, the free energy barrier, calculated as the free energy difference between the dimeric  $[\text{Ru}-\text{O} \cdots \text{O}-\text{Ru}]^{2+}$  TS and two separated  $[\text{Ru}(\text{V})=\text{O}]^+$  species, increases from 18.0 kcal/mol for **4**:**4** (see Figure 4), to 20.7 kcal/mol for **1**:**1**, to 24.5 kcal/mol for **4**:**5**, in very good qualitative agreement with the experimental trend. Transition state structural analysis of **1**:**1** and **4**:**4** also evidences shorter distances between the tips of the axial ligands in the **4**:**4** TS (3.24 Å) compared to the **1**:**1** TS (3.54 Å), suggesting that stronger stacking, stabilizes the **4**:**4** TS relative to the **1**:**1** TS (see Figure S30.). To have additional support for this hypothesis, the stacked axial ligands were rigidly extracted from **4**:**4** TS and **1**:**1** TS, and their interaction energy was calculated. This results in a stacking interaction energy of 6.5 kcal/mol for the MeO-Isoq dimer, while for the unsubstituted Isoq dimer the stacking energy amounts to 3.5 kcal/mol only. Natural population analysis indicates that the increased stacking energy of the MeO-Isoq dimer is due to stabilizing electrostatic interaction between the positively charged C atom bearing the OMe substituent on one

MeO-Isoq ligand, and negatively charged C atoms of the other MeO-Isoq ligand, see Figure S31. This arrangement therefore has a favorable off-center-parallel stacking geometry between aromatic units.<sup>[6]</sup> In addition, analysis of the steric maps of the monomeric species  $[\text{Ru}(\text{V})=\text{O}]^+$ , see Figure S32, clearly indicates that the Me-bpy<sup>+</sup> ligands in **5**, are also destabilized by the higher steric hindrance between the Me-bpy<sup>+</sup> ligands. Steric hindrance is instead negligible in the  $[\text{Ru}(\text{V})=\text{O}]^+$  species **1** and **4**, see again Figure S32.

Finally under extreme conditions (entry 4, Table 1) the system **4** 50  $\mu\text{M}$ /Ce(IV) 350 mM, yields an impressive maximum velocity of oxygen generation of 23.07  $\mu\text{mols s}^{-1}$  which implies a  $\text{TOF}_{\text{max}}$  of 923 cycles/s, which is among the highest reported for a molecular WOC.<sup>7</sup>

In conclusion convergent chemical, electrochemical and DFT experiments involving Ru-bda type catalysts generates a solid knowledge on these systems regarding the key factors that influence their reactivity. This knowledge in turn allows the judicial design of systems for extremely fast water oxidation reactivity, as is the case of **4**, which is vital for the building up of efficient photoanodes.

## Experimental Section

**Materials:**  $\text{RuCl}_3 \cdot 3\text{H}_2\text{O}$  and 6-methoxyisoquinoline were supplied by Precious Metals Online PMO Pty Ltd and Apollo Scientific. All other reagents were purchased from Sigma-Aldrich. 6,6'-Dicarbonixilic acid-2,2'-dipyridyl ( $\text{H}_2\text{bda}$ ),<sup>[4]</sup>  $[\text{RuCl}_2(\text{DMSO})_4]$ <sup>[8]</sup> and [1-Methyl-4,4'-bipyridinium] $\text{PF}_6$  (Me-bpy( $\text{PF}_6$ ))<sup>[9]</sup> were prepared according to the reported procedures. Methanol (MeOH) was distilled over  $\text{Mg}/\text{I}_2$ . All synthetic manipulations under  $\text{N}_2/\text{Ar}$  were performed using standard Schlenk tubes and vacuum-line techniques.

**Synthesis of 4:** The procedure was modified from a previously reported procedure.<sup>[4]</sup>  $[\text{RuCl}_2(\text{DMSO})_4]$  (100 mg, 0.21 mmol), 6,6'-dicarbonixilic acid-2,2'-dipyridyl

( $\text{H}_2\text{bda}$ ) (59.50 mg, 0.2 mmol) and  $\text{Et}_3\text{N}$  (0.1 mL) were dissolved in anhydrous MeOH (10 mL) and heated to reflux for 3 hours under Ar. 6-methoxyisoquinoline (65 mg, 0.41 mmol) was subsequently added to the solution and the reaction was then heated to reflux overnight. The product precipitated as a brown powder, which was filtered, washed with acetone (3 x 15 mL) and diethyl ether (3 x 15 mL) and dried under vacuum (20 mg, 18% yield based on Ru). <sup>1</sup>H NMR (400 Hz, [d4]-methanol):  $\delta$  = 3.91 (6H, s), 7.19 (2H, d,  $J$ =2.3 Hz), 7.23 (2H, dd,  $J$ =2.3, 9.0 Hz), 7.50 (4H, q,  $J$ =7.58 Hz), 7.75 (2H, d,  $J$ =9.0 Hz), 7.92 (2H, t,  $J$ =7.9 Hz), 8.05 (2H, dd,  $J$ =0.9, 7.9 Hz), 8.42 (2H, s), 8.66 (2H, dd,  $J$ =0.9, 7.9 Hz). <sup>13</sup>C NMR (500Hz, [d4]-methanol)  $\delta$  = 28.0, 102.5, 119.5, 120.4, 123.2, 123.6, 124.4, 127.5, 130.1, 136.1, 141.4, 153.2, 154.8, 159.1, 161.4, 172.7. UV-vis [ $\lambda_{\text{max}}$ , nm ( $\epsilon$ ,  $\text{M}^{-1} \text{cm}^{-1}$ ): 237 (122000), 300 (37000) and 400 (16000).  $E_{1/2}$  (MeOH/Acetone 1:1, 0.1M TBAPF<sub>6</sub>): 0.10 V vs Hg/Hg<sub>2</sub>SO<sub>4</sub>. MALDI<sup>+</sup>-HRMS  $m/z$ : Calc for  $\{(\text{MeOIsoq})_2\text{Ru}(\text{bda})\}^+$ : 662.0734, found: 662.0811 (12 ppm). *Anal.* Calc. for **4**·3.5H<sub>2</sub>O ( $\text{C}_{32}\text{H}_{31}\text{N}_4\text{O}_{9.5}\text{Ru}$ ): C, 53.04%; H, 4.31%; N, 7.73%. Found: C, 52.96%; H, 3.97%; N, 7.61%.

**Synthesis of 5:** The procedure was modified from a previously reported procedure.<sup>[4]</sup>  $[\text{RuCl}_2(\text{DMSO})_4]$  (75 mg, 0.17 mmol), 6,6'-dicarbonixilic acid-2,2'-dipyridyl ( $\text{H}_2\text{bda}$ ) (50.6 mg, 0.17 mmol) and  $\text{Et}_3\text{N}$  (0.1 mL) were dissolved in anhydrous MeOH (6 mL) and heated to reflux for 3 hours under Ar. [1-Methyl-4,4'-bipyridinium] $\text{PF}_6$  ([Me-bpy] $\text{PF}_6$ ) (100 mg, 0.31 mmol) was subsequently added to the solution and then heated to reflux overnight. A brown solid (95mg) precipitated as a brown powder, which was filtered, washed with MeOH (3 x 5 mL) and diethyl ether (3 x 15mL) and allowed to dry in air. The dry precipitated was dissolved in 80 mL of 1:1 MeOH/acetone and evaporated to a final volume of 10 mL. Then 40 mL of MeOH were added and the solvent evaporated until precipitation occurred. The suspension was filtered and the solid washed with MeOH (10 mL) and diethyl ether (3 x 15 mL) and finally dried under vacuum (45 mg, 27% yield based on Ru). <sup>1</sup>H NMR (400Hz, [d4]-

methanol):  $\delta$ =7.92 (4H, dd, J=1.5, 5.4 Hz), 8.15 (4H, m), 8.32 (4H, dd, J=1.36, 5.4 Hz), 8.55 (4H, d, J=6.8 Hz), 8.86 (2H, dd, J=1.5, 7.5 Hz), 9.17 (4H, d, J=6.8 Hz).  $^{13}\text{C}$  NMR (500Hz, [d4]-methanol)  $\delta$  = 46.1, 121.5, 124.1, 124.3, 124.6, 131.6, 140.3, 144.95, 150.6, 152.5, 154.7, 158.5, 171.9. UV-vis [ $\lambda_{max}$ , nm ( $\epsilon$ ,  $\text{M}^{-1} \text{cm}^{-1}$ ): 250 (50000), 300 (29000), 510 (16800).  $E_{1/2}$  (MeOH/acetone 1:1, 0.1 M TBAPF<sub>6</sub>): 0.17 V vs Hg/Hg<sub>2</sub>SO<sub>4</sub>. MALDI<sup>+</sup>-HRMS m/z: Calc. for {[Ru(bda)(MeBpy)<sub>2</sub>]PF<sub>6</sub>-dctb}<sup>+</sup>: 1081.2322, found: 1081.2314 (1ppm). Anal. Calc. for 5·2H<sub>2</sub>O (C<sub>34</sub>H<sub>32</sub>F<sub>12</sub>N<sub>6</sub>O<sub>6</sub>P<sub>2</sub>Ru): C, 40.37%; H, 3.19%; N, 8.31%. Found: C, 40.14%; H, 2.76 %; N, 8.11 %.

### Acknowledgements.

CR thanks the European Commission and Marie Curie Actions for an Intra-European Fellowship. AL thanks MINECO CTQ-2013-49075-R and “La Caixa” foundation for financial support. M.R. thanks “La Caixa” foundation for a PhD grant. XS thanks MINECO CTQ2011-26440 for financial support. LC thanks King Abdullah University of Science and Technology for financial support. AP thanks the Spanish MINECO for a Ramón y Cajal contract (RYC-2009-05226) and European Commission for a Career Integration Grant (CIG09-GA-2011-293900).

**Keywords:** Ru complexes, water splitting, supramolecular interactions, redox catalysis, water oxidation catalysis, supramolecular catalysis, DFT calculations

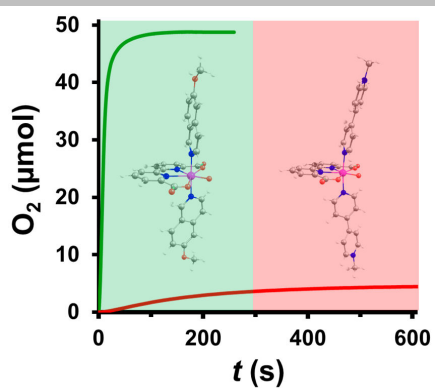
[1] “Molecular Water Oxidation Catalysis: A Key Topic for New Sustainable Energy Conversion Schemes.” Edited by A. Llobet. **2014** John Wiley and Sons Ltd. ISBN: 9781118413371.

- [2] a) S. Neudeck, S. Maji, I. Lopez, S. Meyer, F. Meyer, A. Llobet, *J. Am. Chem. Soc.* **2014**, *136*, 24-27. (b) I. López, M. Z. Ertem, S. Maji, J. Benet-Buchholz, A. Keidel, U. Kuhlmann, P. Hildebrandt, C. J. Cramer, V. S. Batista, A. Llobet, *Angew. Chem. Int. Ed.* **2014**, *53*, 205-210.
- [3] a) L. Duan, L. Wang, A. K. Inge, A. Fischer, X. Zou, L. Sun, *Inorg. Chem.* **2013**, *52*, 7844-7852. b) L. Duan, F. Bozoglian, S. Mandal, B. Stewart, T. Privalov, A. Llobet, L. Sun, *Nat. Chem.* **2012**, *4*, 418-423.
- [4] a) Y. Gao, X. Ding, J. Liu, L. Wang, Z. Lu, L. Li, L. Sun, *J. Am. Chem. Soc.* **2013**, *135*, 4219-4222; b) F. Li, B. Zhang, X. Li, Y. Jiang, L. Chen, Y. Li, L. Sun, *Angew. Chem. Int. Ed.* **2011**, *50*, 12276-12279; *Angew. Chem.* **2011**, *123*, 12484-12487.
- [5] a) C. Di Giovanni, L. Vaquer, X. Sala, J. Benet-Buchholz, A. Llobet, *Inorganic Chemistry* **2013**, *52*, 4335-4345; b) N. Planas, G. Christian, S. Roeser, E. Mas-Marza, M.-R. Kollipara, J. Benet-Buchholz, F. Maseras, A. Llobet, *Inorg. Chem.* **2012**, *51*, 1889-1901.
- [6] C. R. Martinez, B. L. Iverson, *Chem. Sci.* **2012**, *3*, 2191-2201.
- [7] (a) H. Lv, J. Song, Y. V. Geletii, J. W. Vickers, J. M. Sumliner, D. G. Musaev, P. Kögerler, P. F. Zhuk, J. Bacsá, G. Zhu, C. L. Hill, *J. Am. Chem. Soc.* **2014**, *136*, 268–9271. (b) L. Wang, L. Duan, Y. Wang, M. Ahlquist, L. Sun, *Chem. Commun.*, **2014**, web.
- [8] I. P. Evans, A. Spencer, G. Wilkinson, *J. Chem. Soc., Dalton Trans.* **1973**, 204-209.
- [9] E. H. Yonemoto, R. L. Riley, Y. I. Kim, S. J. Atherton, R. H. Schmehl, T. E. Mallouk, *J. Am. Chem. Soc.* **1992**, *114*, 8081-8087.

Entry for the Table of Contents (Please choose one layout)

COMMUNICATION

Supramolecular interactions  
boost water oxidation  
turnover frequencies in Ru-  
bda type of complexes



Craig J. Richmond,<sup>[a]</sup> Roc  
Matheu,<sup>[a]</sup> Albert Poater,<sup>[b]</sup>  
Laura Falivene,<sup>[c]</sup> Jordi Benet-  
Buchholz,<sup>[a]</sup> Xavier Sala,<sup>\*,[d]</sup> Luigi  
Cavallo,<sup>\*,[c]</sup> and Antoni  
Llobet,<sup>\*,[a],[d]</sup>

Page No. – Page No.

**Supramolecular Water  
Oxidation with Ru-bda Based  
Catalysts**